Comparative NO$_2$ Sensing Characteristics of SnO$_2$:WO$_3$ Thin Film Against Bulk and Investigation of Optical Properties of the Thin Film

Haidar jwad Abdul-Ameer [1*]   *Muthafar F. AL-Hilli* [2]   *Mohammed K. Khalaf* [3]

Abstract:

A comparative investigation of gas sensing properties of SnO$_2$ doped with WO$_3$ based on thin film and bulk forms was achieved. Thin films were deposited by thermal evaporation technique on glass substrates. Bulk sensors in the shape of pellets were prepared by pressing SnO$_2$:WO$_3$ powder. The polycrystalline nature of the obtained films with tetragonal structure was confirmed by X-ray diffraction. The calculated crystalline size was 52.43 nm. Thickness of the prepared films was found 134 nm. The optical characteristics of the thin films were studied by using UV-VIS Spectrophotometer in the wavelength range 200 nm to 1100 nm, the energy band gap, extinction coefficient and refractive index of the thin film were 2.5 eV , 0.024 and 2.51, respectively. Hall measurements confirmed that the films are n-type. The NO$_2$ sensing characteristics of the SnO$_2$:WO$_3$ sensors were studied with various temperatures and NO$_2$ gas concentrations. Both thin film and bulk sensors showed maximum sensitivity at temperature of 250 $^{\circ}$C. Thin film sensors showed enhanced response in comparison to that of pellets.

Keywords: WO$_3$ doped SnO$_2$; Thin Films; Pellets; NO$_2$ Gas Sensor; XRD; UV-Vis Spectrometry.

Introduction:

Environmental safety strategy in most countries focused on the regulation, accurate measurement and control of the toxic gases such as H$_2$S, O$_3$, CO, H$_2$ and NO$_2$ in the atmosphere. Nowadays, air contamination by nitrogen oxides (NO$_x$), mostly NO and NO$_2$, is becoming a remarkable environmental topic. Nitrogen dioxide (NO$_2$) is a noxious compound with a bitter odor that is dangerous to the environment as a main reason of acid rain and photochemical smog. NO$_2$ is mostly formed by power plants, combustion engines and automobiles. It can also prompt health difficulties, such as olfactory paralysis. Protection guidelines recommend that humans should not be exposed to more than 3ppm NO$_2$ gas for time longer than 8 hours. NO$_2$ accompanying with other pollutants such volatile organic compounds (VOC) is responsible for the creation of ozone. So, it is very required to develop a dependable sensor that can efficiently detect NO$_2$ even with exceedingly low concentration (1- 3).

[1]Ministry of Education, Baghdad, Iraq.
[2]Department of Physics, College of Science, University of Baghdad, Baghdad, Iraq.
[3]Ministry of Science and Technology, Department of Materials Researches, Applied Physics Center, Baghdad, Iraq.
[*]Corresponding Author: haydarjwad2@yahoo.com

The SnO$_2$ is a semiconductor material extremely transparent and with elevated mechanical and chemical stability, excluding for their interactions with oxygen atoms at high temperature. In addition to its high optical transmission owing to a wide optical band gap approximately 3.8 eV, SnO$_2$, thin films have high n-type conductivity, which is because of their non-stoichiometric character related with oxygen vacancies and interstitial tin in the lattice (4-6). The conductivity could be changed from regular semiconducting to degenerate one via properly doping the material and maneuvering the oxygen deficient sites (7). Through the past few decades, SnO$_2$ has been broadly applied in a wide range of significant applications, such as solid-state gas sensors, liquid crystal displays, thin-film heaters, photovoltaic cells, optical coatings, self-cleaning materials and transparent conducting electrodes (8, 9). It is a fact that the sensor properties can be changed by varying the crystal structure, dopants, preparation method, operation temperature: etc (10-12).

Gas sensors work on the principle of a change in electrical conductance on exposure to the gas which is to be detected (13). The conductivity of SnO$_2$ sensor rises in the existence of a reducing gases (like CO), and reductions in the existence of an oxidizing gas (like O$_2$) (14). The structural order and the surface morphology of the material are chief

reasons to operate as sensor; therefore, WO_3 doped gas sensors have particular significance due to structural order of WO_3 (15, 16). In this paper, the influence of the operating temperatures over the sensitivity measurements of the films as well as bulk samples are discussed.

The aim of this work is to design a reliable NO_2 gas sensor for environmental protection with high sensitivity, fast response time and fast recovery time from semiconductor metal oxide.

Materials and Methods:

The chemicals SnO_2 and WO_3 in powder form were obtained from (Ferak, Germany, 99.99 % pure) and (The British Drug Houses, England, 99.99 % pure), respectively. 1 % weight of WO_3 powder in SnO_2 have been mixed uniformly and made fine by grinding in mortar with pestle for 1 hour. Then the powders were sintered at 900 ℃ for 2h and utilized for sensor fabrication. Thin films were prepared by thermal evaporation technique onto ultrasonically and chemically cleaned glass substrates. Film thickness was measured by optical interference method employing a (Angstrom Sun Technologies Inc. SR 300 Spectrometer) and was found to be 134 nm. Bulk sensors in the shape of pellets were prepared by pressing $SnO_2:WO_3$ powder using die of 15 mm diameter and uniaxial hydraulic press. Al grid were deposited through a mask on front surface of the prepared sensors. Electrical contacts were made by silver paste. The crystal structures of the film was measured by X-ray diffraction (XRD) using a (Shimadza XRD -6000) diffractometer, employing CuK_α (1.54 Å) radiation. The optical and electrical characteristic of the films were done by uv-vis spectrometer (Shimadzu uv-1800) and Hall measurement system (Ecopia HMS-3000), respectively.

The sensitivity exams were performed in a closed chamber containing a heating element. The samples were connected to a multimeter (Victor 86 B) and a constant voltage source in order to measure the resistance. The sample temperature was observed and organized by a thermocouple (K-type) joined to the substrate. The sensor response was measured as a function of temperature.

Different concentrations of NO_2 gas (110, 165 and 220 ppm) were inserted into the testing chamber by adjusted leaks through needle valves. A pirani gauge with a rotary pump was utilized to regulator the flow of objective gas in the testing chamber.

The sensor response is defined as (1):

$$S = \frac{R_g - R_a}{R_a} \qquad (1)$$

Where, R_a and R_g are the sensor resistances in the existing of atmospheric air and objective gas, respectively.

Time period over which sensor resistance decreases to 10% of the saturation value when the objective gas is switched off and the sensor is placed in artificial (or reference) air is the recovery time.

Results and Discussions:

The XRD configuration of $SnO_2:WO_3$ thin film is shown in fig. 1. It is clear that the film is polycrystalline in structure. Matching of the observed and of the standard (hkl) planes confirms that the deposited film has a primitive tetragonal structure (17). The film shows a preferred orientation along the (110) plane. The (100), (101), (200), (211), (220) and (310) peaks coincide well with standard data (JCPDS Card No.88-0287) (18). The crystallite size of film was calculated by Debye-Scherrer's formula given by (4):

$$D = 0.9\, \lambda/\beta\cos\theta \qquad (2)$$

Where λ is the wavelength of X-ray radiation (1.54 Å), β is the full width half maximum (FWHM) of the peak. The rate crystallite size is found to be 52.43 nm. Our results are in close agreement with Tripathy and Hota (10, 19).

Optical analysis of $SnO_2:WO_3$ thin films on glass substrates was performed from transmission percentage versus wavelength curve in the wavelength scope 200 nm to 1100 nm, which is presented in fig. 2. The sensitivity is highly dependent on the optical properties of the film. The film exhibits a very elevated transmission (>80%) in the visible part owing to the fact that the reflectivity is low and there is low absorption because of excitation of electrons from the valence band to conduction band (20). The films demonstrate an abrupt fundamental absorption edge at about 400 nm. The existence of clear interference fringes configuration in the optical transmittance spectra shows the growth of good quality thin films without any sort of in homogeneity which confirms that $SnO_2:WO_3$ thin films possess semiconducting properties as it was recognized by Nowak that the pure semiconducting compounds have an abrupt absorption edge (21). In order to get the band gap, the absorption coefficient (α) was calculated from the transmission data via using the following relation (22):

$$\alpha = \frac{\ln\frac{1}{T}}{t} \qquad (3)$$

Where t is the film thickness and T is the transmittance. The value of absorption coefficient (α) is 6280 cm^{-1} as shown in fig. 3. For the direct transition, the optical band gap energy of film was specified by using the equation (22),

$$\alpha = A\,(h\nu - E_g)^{1/2}/h\nu \qquad (4)$$

Where A is the corresponding absorption constant, $h\nu$ is the photon energy and E_g is the optical band gap. From the plot of $(\alpha h\nu)^2$ vs. $h\nu$ the band gap is

specified by extrapolating the straight line portion of the plot to the energy axis. The cut off on energy axis provides the value of band gap energy which was found to be 2.5 eV as demonstrated in fig. 4. The extinction coefficient (k) value of film was determined from (23) :

$$k = \alpha\lambda/4\pi \qquad (5)$$
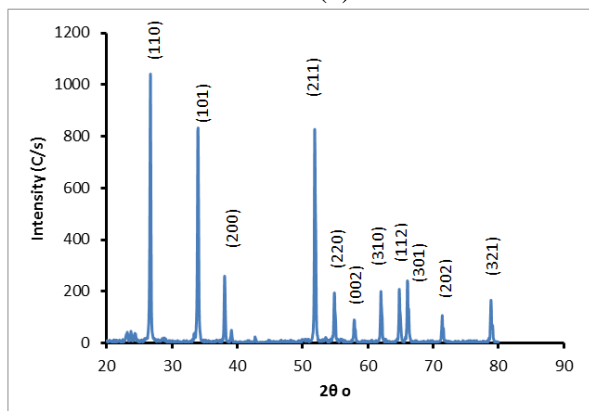
Figure 1. XRD pattern of SnO$_2$:WO$_3$ thin film.
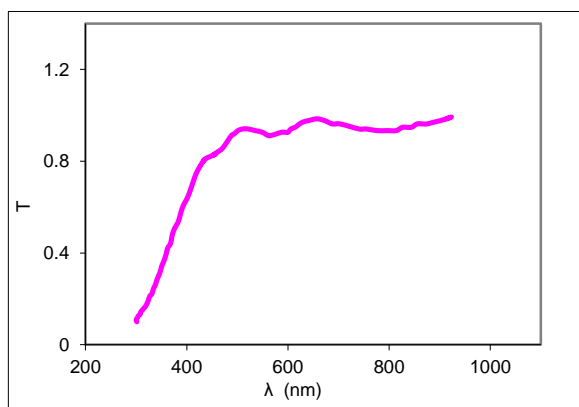
Figure 2. Transmittance spectra of SnO$_2$:WO$_3$ thin film.
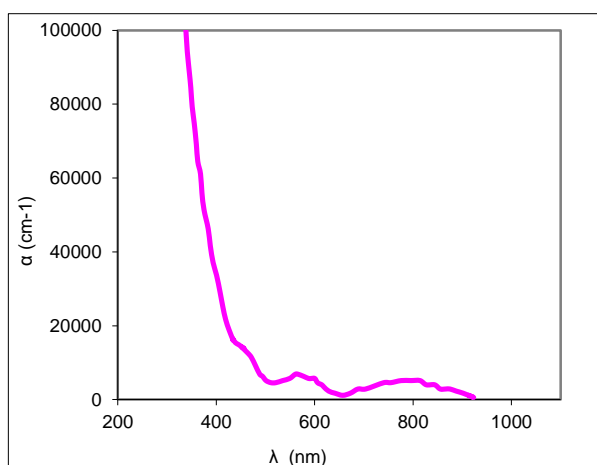
Figure 3. Absorption coefficient vs wavelength of SnO$_2$:WO$_3$ thin film.
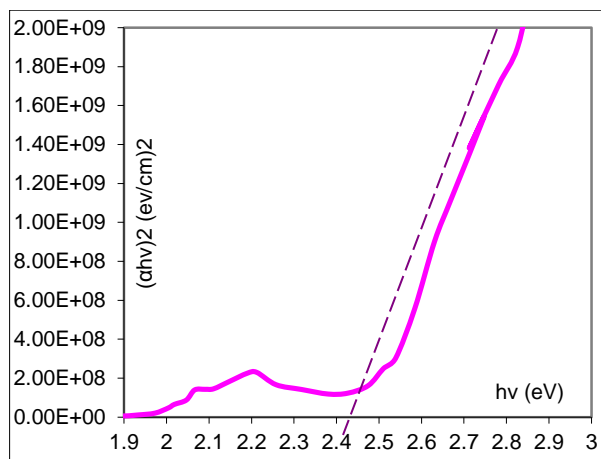
Figure 4. ($\alpha h\nu$)^2 vs. hν of SnO$_2$:WO$_3$ thin film.

and was found to be 0.024 at the wavelength 496 nm as manifested in Fig. 5.

The extinction coefficient is related to the creation of defects and absorption centers. The refractive index was calculated from the following equation (24) :

$$n = \left[\frac{4R}{(R-1)^2} - k^2\right]^{1/2} - \frac{(R+1)}{(R-1)} \qquad (6)$$

and was found to be 2.51 as revealed in fig. 6. Nearly similar result is given by K. S. Muhamed and N. R. Muhammed (14). The elevated value of the refractive index may possibly because of high porosity and surface roughness of the films, which is chiefly referred to larger grain size. Sensitivity of thin semiconducting film is extremely reliant on film porosity, film thickness, operating temperature, existent of additives, and crystallite size. However porosity is estimated to have a large influence on sensor sensitivity (10).

The Hall effect measurement revealed that the Hall coefficient, the carrier concentration and the mobility of the films are -1.065x10^{10} cm^3/C, -5.863X10^8 cm^{-3} and 2.725 cm^2/V.sec, respectively. The negative sign of the Hall coefficient value exhibits the n-type semiconducting nature of the films. Our result concerning the mobility is in agreement with the study performed by Songqing (8).

It is well recognized that gas sensing is a surface phenomenon and is chiefly organized by the adsorbed oxygen species (25). Doping with WO$_3$ provides rise to several oxygen species and surface states which lead to enrichment in the gas sensing (7). The fundamental gas sensing properties of the SnO$_2$:WO$_3$ thin films and bulk tablets were investigated as a function of operating temperature and test gas concentration. In this study the films were characterized by many factors like sensitivity, response and recovery time. Figure 7 shows the sensitivity to NO$_2$ gas as a function of operating temperature for thin film and bulk. It is clear that

the maximum sensitivity occurs at temperature of 250°C (26, 27). At low temperatures there is fewer oxygen coverage, when the sensor is exposed to air and thus when target gases are inserted, there is an insignificant variation in sensitivity. As the operating temperature increases, the number of adsorbed oxygen species would have reacted more and more number of electrons which are released due to this reaction sent back to conduction band i.e., desorption average of adsorbed gases increases with increasing temperatures too. As temperature increases further, more and more adsorb oxygen species reacted and more and more electrons sent back to conduction band leading to increase in conductivity. At 225°C , which is known as critical temperature T_C, almost all the adsorb oxygen species reacted and maximum electrons sent back to conduction band leading to maximum sensitivity. The reduction in sensitivity for temperatures over a critical operating temperature, T_C , can be referred to the higher desorption rates at these temperatures. When target gases are inserted , the added desorption owing to the target gases is small relative to the steady-state desorption in air, directing to reducing effect on the sensor response for $T > T_C$. The results indicated that the thin film structure has a higher sensitivity than those produced by pellet bulk structure, owing to a larger active surface area of nanostructure, which can offer more active space for the interaction between SnO_2:WO_3 and target gases.
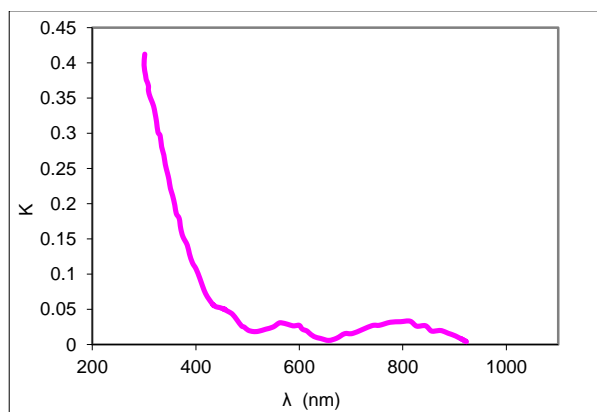
Figure 5. Extinction coefficient vs wavelength of SnO_2:WO_3 thin film.
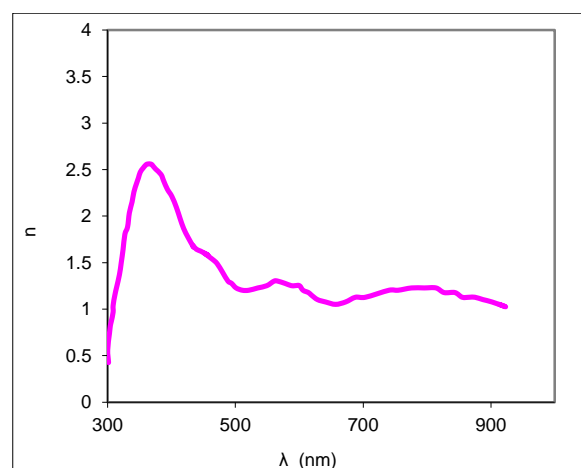
Figure 6. Refractive index vs wavelength of SnO_2:WO_3 thin film.
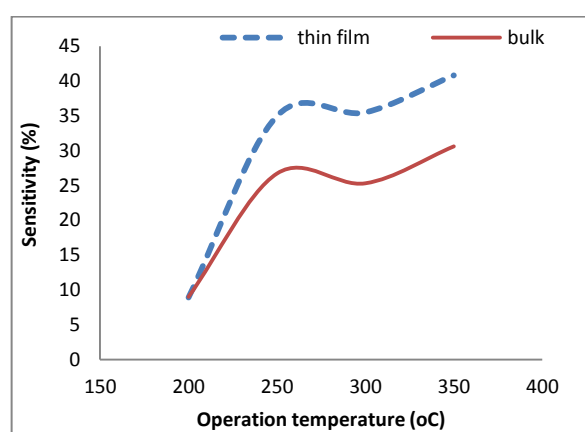
Figure 7. Sensitivity vs. operating temperature for SnO_2:WO_3 thin film and bulk.

Smaller grain size in the nanocrystalline material lowers the activation energy and the existence of dispersed W nanocluster over the SnO_2 surface additional reduced the activation energy. This is the reason of lowering the operating temperature of the SnO_2:WO_3 sensor. However, high surface to volume ratio can be obtained not only by reducing grain size, but also by highly-ordered porous structure (28- 30). Our result is nearly in agreement with Shi *et al*.(31).

The sensitivity of the thin film for 110, 165 and 220 ppm of NO_2 gas concentration at 250 ℃ against working time is represented in fig. 8. It is detected that the sensitivity rises linearly as the NO_2 concentration increases from 110 ppm to 220 ppm. The linear correlation between the sensitivity and the NO_2 concentration may be because of the availability of adequate number of sensing positions on the film to perform upon the NO_2. The sensitivity at gas concentration below 165 ppm was very low. The response time at gas concentration 165 ppm was around 4 sec and at gas concentration 220 ppm was 2 sec while the recovery time were 50 sec and 120 sec, respectively. Since SnO_2:WO_3 films are n-type semiconductor, the oxidizing NO_2

molecules adsorbed on the oxide surface could captivate electrons shape the conduction band and form NO_2 (32- 34). Our result is nearly similar to that obtained by Bari and Patil (35).

Figure 9 illustrates the response time change with operating temperature. The response time for thin film sensor at low operating temperatures was found to be lower than that of bulk sensor. While at higher temperatures the bulk sensor showed lower response time. In the present work the response time is directly associated to the grain size and the size of the particle boundary in the sensor material.

Figure 10 shows the recovery time versus operating temperature for thin film and bulk gas sensors. The thin film sensor recovery time increased with temperature up to 300°C, and then starts to decrease. While the peak operating temperature for bulk sensor exceeds the maximum testing temperature at 400°C.

The sensor could be used to observe NO_2 gas levels in exhausts at ppm concentrations.

Conclusion:

The influence of the operation temperature and gas concentration over the gas sensing characteristics of SnO_2:WO_3 in thin film and bulk form have been examined. XRD study revealed that the obtained films were polycrystalline with tetragonal structure and the crystalline size to be 52.43 nm. Optical transmittance measurements denote that the deposited thin films have band gap energy equal to 2.5 eV which confirm that these are good semiconducting films. The n-type nature of the films detected from negative sign of the Hall coefficient. These sensors were studied for NO_2 gas sensing and exhibited high sensitivity and fast response and recovery times. The response time for thin film sensor at low operating temperatures was found to be lower than that of bulk sensor, while at higher temperatures the bulk sensor showed lower response time. Thin film is a superior in comparison to bulk for sensitivity measurement. SnO_2 doping by WO_3 is very operative for improving the gas sensing properties of SnO_2. The results denote that the SnO_2:WO_3 sensors are hopeful for manufacturing applications.
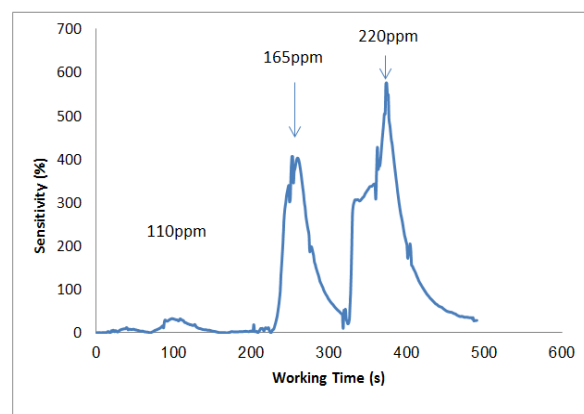
Figure 8. Sensitivity vs. working time for SnO_2:WO_3 thin film at different gas concentrations at 250 ℃
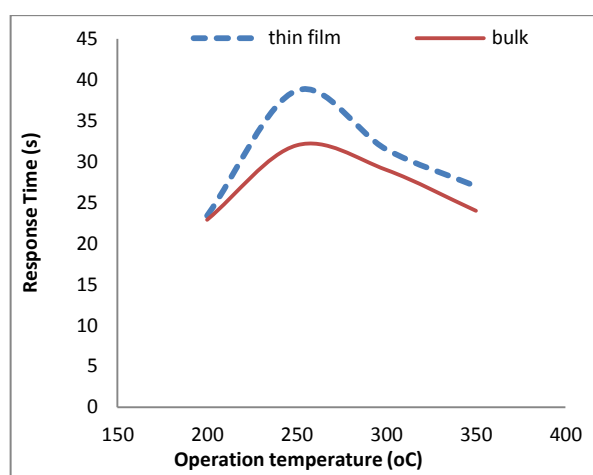
Figure 9. Response time vs. operating temperature for SnO_2:WO_3 thin film and bulk.
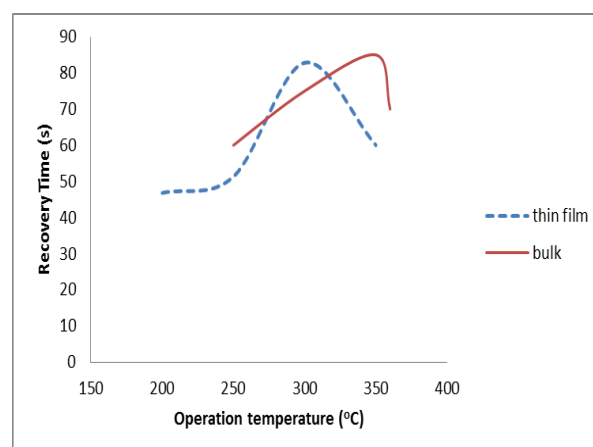
Figure 10. Recovery time vs. operating temperature for SnO_2:WO_3 thin film and bulk.

Conflicts of Interest: None.

References:
1. Sharma A, Tomar M, Gupta V. SnO_2 thin film sensor with enhanced response for NO_2 gas at lower temperatures, Sensors and Actuators B: Chemical. 2011;156: 743-752.

2. Chen C, Lin S, Lin T, Hsu C, Hsueh T, Shieh T. The assessment for sensitivity of a NO₂ gas sensor with ZnGa₂O₄/ZnO core-shell nanowires-a novel approach. Sensors, 2010; 10:3057-3072.

3. Garde A. Gas sensing properties of WO₃ thick film resistors prepared by screen printing technique, Int. J. Chem. Phys. Sci. 2016;5(3): 1-13.

4. Kocyigit A, Tatar D, Battal A, Ertugrul M, Duzgun B. Highly efficient optoelectronic properties of doubly doped SnO₂ thin film deposited by spin coating technique. J. Ovonic Res. 2012;8(6): 171-8.

5. Nagirnyak S, Dontsova T. Effect of modification/doping on gas sensing properties of SnO₂. Nano Res. Appl., 2017;3(2:8): 1-5.

6. Nagirnyak S, Lutz V, Dontsova T, Astrelin I. The effect of the synthesis conditions on morphology of tin (IV) oxide obtained by vapor transport method. Springer Proc Phys, 2016;183:331-341.

7. Boshta M, Mahmoud F A, and Sayed M H. Characterization of sprayed SnO₂: Pd thin films for gas sensing applications. Journal of Ovonic Research, 2010;6(2): 93-98.

8. Songqing Z, Yueliang Z, Shufang W, Kun Z , Peng H. Effect of ambient oxygen pressure on structural, optical and electrical properties of SnO₂ thin films. Rare Metals. 2006;25(6): 1-4.

9. Das S and Jayaraman V. SnO₂: A comprehensive review on structures and gas sensors. Prog. Mater. Sci. 2014;66: 112-255.

10. Tripathy S K , Hota B P. Carbon monoxide sensitivity of tin oxide thin film synthesized by sol gel method, The African Review of Physics. 2012;7(0047): 401-6.

11. Dontsova TA, Nagirnyak SV, Zhorov VV Yasiievych YV. SnO₂ nanostructures: Effect of processing parameters on their structural and functional properties. Nanoscale Res Lett, 2017;12: 1-7.

12. Smulko J, Trawka M, Granqvist CG, Ionescu R, Annanouch FE. New approaches for improving selectivity and sensitivity of resistive gas sensors: A review, Proc of the 8th Intern Conf of Sensing Techn, Liverpool, UK. 2014: 13-18.

13. Sohn J C, Kim S E, Kim Z W, Yu Y S. H₂S gas sensing properties of SnO₂: CuO thin film sensors prepared by e-beam evaporation. Trans. Electr. Electron. Mater.(Online), 2009;10(4): 135-9.

14. Muhamed S K, Muhammed R N. Growth, structural, optical, morphological studies of SnO₂ thin films prepared by spray pyrolysis technique. IJIRSET., 2015;4(5): 3274-8.

15. Dhannasare S B, Yawale S S, Unhale S B, Yawale S P. Application of nanosize polycrystalline SnO₂-WO₃ solid material as CO₂ gas sensor. Revista Mexicana de Física. 2012;58: 445-450.

16. Li C, Lv M, Zuo J , Huang X. SnO₂ highly sensitive CO gas sensor based on quasi-molecular-imprinting mechanism design, Sensors. 2015;15: 3789-3800.

17. Rieu M, Camara M, Tournier G, Viricelle JP, Pijolat C, Rooij N F De, Briand D, Fully inkjet printed SnO₂ gas sensor on plastic substrate. Sens. and Actuators B: Chem., 2016;236: 1091-7.

18. Sagadevan S, Podder J. Optical and electrical properties of nanocrystalline SnO₂ thin films synthesized by chemical bath deposition method, Soft Nano. Lett., 2015;5: 55-64.

19. Bhagwat A D, Sawant S S, Ankamwar B G , Mahajan C M. Synthesis of nanostructured tin oxide (SnO₂) powders and thin films by Sol-Gel method, J. Nano Electro. Phys., 2015;7(4): 04037-1 – 04037-4.

20. Rajpure K Y, Kusumade M N, Neumann-Spallart M N, Bhosale C H. Effect of Sb doping on properties of conductive spray deposited SnO₂ thin films, J. Mater. Chem. Phys.2000;64:184-188.

21. Nowak M. Linear distribution of intensity of radiation reflected from and transmitted through a thin film on a thick substrate. Thin Solid Films. 1995;266: 258-262.

22. Zhang X, Li X M, Chen T L, Bian J M , Zhang C Y. Structural and optical properties of Zn₁₋ₓMgO thin films deposited by ultrasonic spray pyrolysis. Thin Solid Films. 2005;492: 248-252.

23. Mohamed S H, El-Hossary F M, Gamal G A, Kahlid M M. Properties of indium tin oxide thin films deposited on polymer substrates. Acta Physica Polonica A. 2009;115(3): 704-708.

24. K. Chopra, Thin film phenomena, (1969) Mc Graw-Hill, USA. PP 733.

25. Nalage S, Mane A, Pawar R, Lee C , Patil V. Polypyrrole-NiO hybrid nanocomposite films: highly selective, sensitive, and reproducible NO₂ sensors. Ionics. 2014;20: 1607-1616.

26. Zappa D, Bertuna A, Comini E, Kaur N, Poli N, Sberveglieri V, Sberveglieri G,. Metal oxide nanostructures: preparation, characterization and functional applications as chemical sensors. Beilstein J. Nanotechnol. 2017;8:1205-17.

27. Zhang J, Zeng D, Zhu Q, Wu J, Huang Q Xie C. Effect of nickel vacancies on the room-temperature NO₂ sensing properties of mesoporous NiO nanosheets, J. Phys. Chem. C. 2016;120: 3936-45.

28. Kamble A S, Pawar R C, Tarwal N L, More L D , Patil P S. Ethanol sensing properties of chemosynthesized CdO nanowires and nanowalls, Mater. Lett. 2011;65: 1488-91.

29. Kamble A S, Pawar RC, Patil J Y, Suryavanshi S S , Patil P S. From nanowires to cubes of CdO: Ethanol gas response, J. Alloy. Compd. 2011;509: 1035-39.

30. Mizsei J, Lantto V. Simultaneous response of work function and resistivity of some SnO₂-based samples to H₂ and H₂S. Sens. Actuators B: Chem. 1991;4(1-2): 163-68.

31. Shi L Q, Gao W, Hasegawa y, Katsube T, Nakano M , Nakamura K. Highly sensitive SnO₂-based gas sensor for indoor air quality monitoring, Proceedings: Indoor Air. 2005; 3385-88.

32. Sadek A Z, Choopum S, Wlodarski W, Ippolito S J , Kalantar-zadeh K. Characterization of ZnO nanobelt-based gas sensor for H₂, NO₂, and hydrocarbon sensing, IEEE Sens. J. 2007;7: 919-24.

33. Khalaf M K, Al-Temmeme N A, Ibrahim F T , Hammed M A. Crystalline structure and surface morphology of tin oxide films grown by DC reactive sputtering, Photonic Sensors. 2014;4: 349-53.

34. Stanoius A, Somacescu S, Calderon-Moreno J M, Teodorescu V S, Florea O G, Sackmann A , Simion C E. Low level NO₂ detection under humid

background and associated sensing mechanism for mesoporous SnO_2, Sens. Actuators, B. 2016;231: 166-74.

35. Bari R H, Patil S B. Low temperature NO_2 sensing performance of nanostructured SnO_2 thin films. Scholars Research Library. 2014;5(6): 1-11.

دراسه مقارنه للخصائص التحسسيه لغاز NO_2 لغشاء رقيق و عينه كتليه من مادة $SnO_2:WO_3$ و أستقصاء الخواص البصريه للغشاء الرقيق

حيدر جواد عبد الأمير [1]   مظفر فؤاد جميل الحلي [2]   محمد خماس خلف [3]

[1] وزارة التربيه، بغداد، العراق
[2] قسم الفيزياء، كلية العلوم، جامعة بغداد، بغداد، العراق
[3] وزارة العلوم و التكنلوجيا، دائرة بحوث المواد، مركز بحوث الفيزياء التطبيقيه

الخلاصة:

تم انجاز بحث مقارن لتحسسية الغاز من مادة $SnO_2:WO_3$ على شكل غشاء رقيق و عينه كتليه . رسبت الأغشيه الرقيقه على ارضيات زجاجيه بتقنية التبخير الحراري. حضرت العينات الكتليه على شكل اقراص بكبس مسحوق $SnO_2:WO_3$. لوحظ من خلال حيود الأشعه السينيه أن الأغشيه متعددة التبلور و تمتلك تركيب رباعي الزوايا وبحجم بلوري يساوي 52.43 nm . وجد أن سمك الأغشيه يساوي 134 nm . تم دراسة الخصائص البصريه للأغشيه الرقيقه بأستخدام مطياف UV-VIS في مدى من الأطوال الموجيه nm (1100-200) ، و كانت قيم كل من فجوة حزمة الطاقه و معامل الخمود و معامل أنكسار الغشاء الرقيق 2.5 eV و 0.024 و 2.51 على التوالي. أكدت قياسات هول أن الأغشيه من نوع n . لقد درست الخصائص التحسسيه لمادة $SnO_2:WO_3$ لغاز NO_2 عند درجات حراريه مختلفه و لتراكيز مختلفه من غاز NO_2 . آظهر كل من الغشاء الرقيق و العينه الكتليه اقصى تحسس عند درجة حرارة 250 °C . آظهرت متحسسات الأغشيه الرقيقه استجابه افضل مقارنة بالأقراص.

الكلمات المفتاحيه: SnO_2 المطعم ب WO_3 ، أغشيه رقيقه، اقراص، متحسس غاز NO_2 ، XRD ، مطياف UV-Vis .